# MODEL PREDICTIVE CONTROL OF THE INDUCTION MOTOR

*A Project Report*

*submitted by*

**ABHISHEK BAKOLIA**

*in partial fulfilment of the requirements*
*for the award of the degree of*

**MASTER OF TECHNOLOGY**

**DEPARTMENT OF ELECTRICAL ENGINEERING**
**INDIAN INSTITUTE OF TECHNOLOGY MADRAS.**

**JULY 2021**

# THESIS CERTIFICATE

This is to certify that the thesis titled **MODEL PREDICTIVE CONTROL OF THE INDUCTION MOTOR**, submitted by **Abhishek Bakolia**, to the Indian Institute of Technology, Madras, for the award of the degree of **Master of Technology**, is a bonafide record of the research work done by him under our supervision. The contents of this thesis, in full or in parts, have not been submitted to any other Institute or University for the award of any degree or diploma.

**Prof. Srirama Srinivas**
Project Guide
Dept. of Electrical Engineering
IIT-Madras, 600 036

Place: Chennai

Date: 20th July 2021

# ACKNOWLEDGEMENTS

I would like to express my sincere gratitude to Prof. Srirama Srinivas for guiding, encouraging and providing me a chance to work under his able guidance. His dedication, keen interest and above all, his overwhelming attitude to help his students has been solely and mainly responsible for completing my work. I consider it an invaluable learning opportunity and pleasure to work on this exciting project under his guidance.

I am very thankful to Mr. Nagasurya Prakash Musunuru. His help was critical in solving many problems that I encountered during the project. I would also, extend my thanks to my M.Tech batch mate Mr. Althurthi Sai Bhargava for his support during my work.

This work could not have come to this stage without the support and encouragement from my parents, siblings, and friends. My heartfelt thanks to all of them.

# ABSTRACT

KEYWORDS: Finite Control Set Model Predictive Control (FS-MPC), Induction Motor, Two level three phase Inverter, Predictive Torque Control

Model Predictive Control (MPC) is introduced in the field of control of Power Electronics and motor drives due to its advanced control techniques. From the past few decades research in the field has been increased with the development of various controller platforms which are required for their implementation. This report presents a detailed explanation of the implementation of the MPC control technique to the power converter and motor drive. A simple classification of MPC, Finite Control Set Model Predictive Control is introduced which is applied to induction motor fed by the two-level three-phase inverter. Among the various FS-MPC strategies, Predictive Torque Control is explained in detail.

This project presents the detailed application of Finite Control Set Model Predictive Control (FS-MPC) on the Induction Motor fed by a two-level three-phase inverter. The explanation of the theory, concepts, methods, and implementation is shown for inverter, induction motor and MPC algorithm with diagrams in every step is documented. PTC predicts the electromagnetic torque and stator current of the induction machine to evaluate the cost function and selects the best switching state which is further fed to the inverter. The results are presented in detail of the different tests performed on induction motor by Predictive Torque Control to test the performance. The implementation of PTC requires a deep understanding of the dynamics of the induction machine to prepare a model to predict the control variables which uses the model of the motor and appropriate cost function to control the torque and flux of the motor. The behavior and performance in the steady and transient state are also discussed.

# TABLE OF CONTENTS

# LIST OF TABLES

# LIST OF FIGURES

# CHAPTER 1

# INTRODUCTION

For the past many decades, power electronics converters and control drives have helped us with various kinds of applications from industrial to residential uses [1]. There has been continuous research in this field to increase the efficiency and performance of power electronics and drives as the widespread application in industries. With the increase in demand for electrical energy with high efficiency and power quality, development has been done in semiconductor devices, converter topologies, and control drives.

The induction motor has gained a lot of importance and wide usage due to its importance in the field of industries, transportation, and common household applications. Induction motor is usually preferred in terms of cost and installation in comparison to DC and synchronous motors. Their construction and robustness make them useful in most situations for a long time as they demand a very low maintenance cost [2]. The speed control of the induction machines is necessary as different applications require the motor to run at a different speed. Therefore proper controlling techniques are required to utilize induction motors for different applications. Pulse width modulation (PWM) has a key role in today's world of power electronics and inverters to control frequency, voltage and maintain lower harmonics for the control of induction motors. A wide range of research has been put to improve the methods of controlling the gating signals of the inverter. The field of digital signal processing has played an important role in the implementation of the controlling algorithms by reducing the cost and complexity [3].

## 1.1 Classical Control Techniques

In the last few decades, to control the electrical drives two control strategies have dominated high-performance applications: Field Oriented Control (FOC) and Direct Torque Control (DTC). Both of these control techniques have been accepted widely [4].

The Field Oriented Control (FOC), introduced in the 1970s bought a revolution in induction motor control [5]. To realize the behavior of the separately excited DC machine, the stator currents are decomposed in the d-axis component for rotor flux and the q-axis component for electromagnetic torque. Both of these currents are regulated by two linear proportional-integral controllers in the synchronously rotating reference frame. The d-axis is aligned to the rotor flux to achieve the decoupled control of the torque and flux. Hence, in the rotatory frame the rotor flux magnitude is controlled by the real part $i_{sd}$ and electromagnetic torque is controlled by imaginary part $i_{sq}$ of the stator current. Finally, to produce the voltage vector the gate pulses are generated by using space vector modulation. A good dynamic flux and torque responses are obtained with constant switching frequency. With the presence of two PI controllers and axis transformation, the control structure of FOC is complex.

Direct Torque Control (DTC) was introduced in the 1980s and emerged as the alternative control strategy to FOC [6]. It has a much simpler complexity as it does not require axis transformation between synchronous and rotatory reference frames and does not require any modulation block. DTC used a predefined switching table based on the stator flux position and error signs of torque and flux to select the best voltage vector for the inverter. It includes two independent hysteresis blocks for controlling torque and flux. This control strategy provides a quick dynamic response but due to the presence of the hysteresis blocks, ripples in torque and flux are produced [7].

## 1.2 Predicitve Control

The increase in the usage of power converters for different applications has given rise to an increase in the research in control strategies. The control techniques of the converters are studied and new control techniques are proposed every year. Some of the control techniques are shown in figure 1.1. Hysteresis and Linear control are the most established control techniques. With the development of powerful microprocessors, more advanced and complex algorithms have emerged such as sliding mode, predictive control, and artificial intelligence. Sliding mode control presents robustness and considers switching states of the power converter [8]. Among all these control techniques, the predictive control technique is the most interesting and advanced alternative as it has several advantages over others which makes it suitable for control of power converters [9]:

- Intuitive and easy to implement the algorithm.
- It can include non-linearities and constraints easily.
- It provides a facility of inclusion and control of multi variables.
- Any modification and extensions can be done according to the requirement of its application.

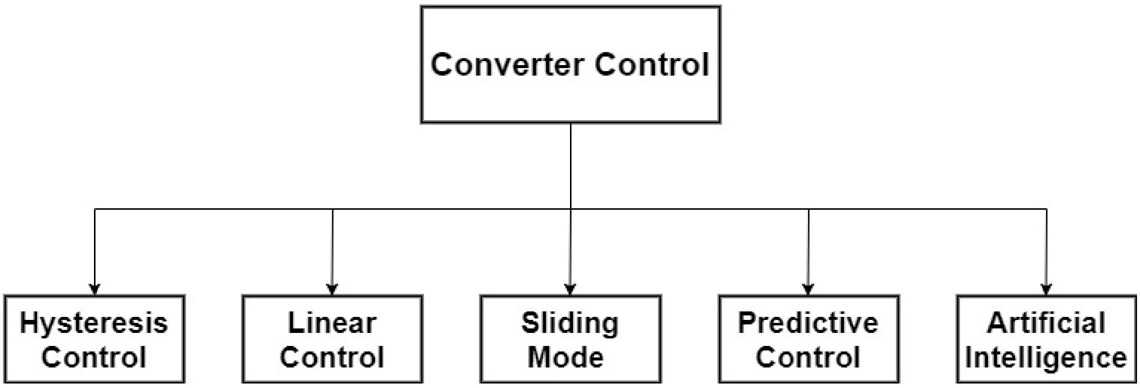

Figure 1.1: Different types of Converter Control Schemes

Although predictive control requires a huge amount of computations as compared to other control schemes, the availability of fast microprocessors has become easier to compute and implement. Predictive Control has a wide variety of control methods and is shown in figure 1.2 [9].

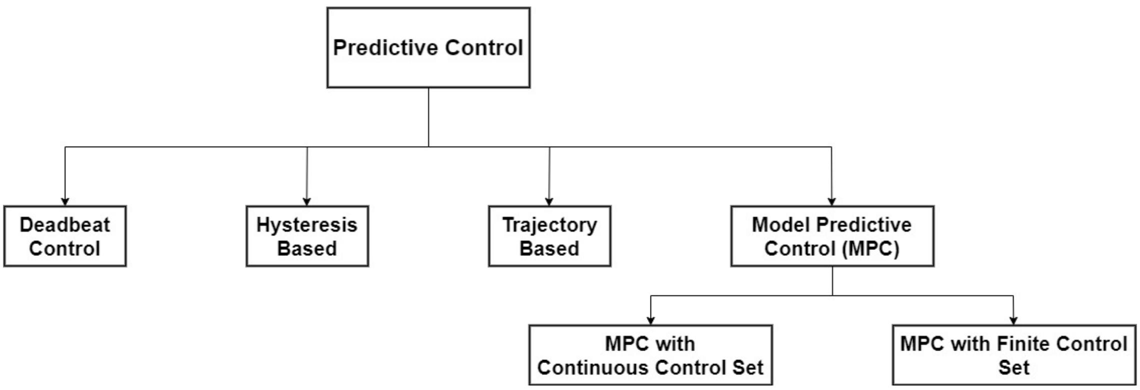

Figure 1.2: Classification of Predictive Control Methods

The basic idea behind predictive control is to predict the future values of the controlling variables of the model of the system. Further, the controller obtains the optimal actuation according to predefined optimization criteria which is different for different predictive control methods. In deadbeat control, the optimal actuation makes the error to zero for every next sampling time [10, 11]. In the hysteresis-based control, the controlling variables are kept within the boundaries of the hysteresis area [12] whereas, in trajectory based control, the controlling variables are forced to follow a predefined trajectory [13]. In this Model Predictive Control, the cost function is evaluated and optimized [1].

## 1.3 Model Predictive Control

Model predictive control (MPC) has been used in the chemical and oil industries since the 1980s where the desired reference does not change frequently. This control technique became popular and later was introduced in power electronics [14-17]. In recent times, MPC for power converters has gained a lot of attention despite high computational due to its capability of handling multivariable, system constraints, and nonlinearities in a very intuitive way [18]. At present time its applications have shown good performances in power converters and high-performance motor drives. The main advantage of the MPC technique is its optimization in current values while keeping in mind future values. The increase in development and advancement of the Digital Signal Processors (DSPs) in past decades has enabled the implementation of MPC in power electronics, such as converters, energy storage and conversion, smart grid, and motor drives [19].

MPC is considered as a wide class of controllers and its main characteristic is to use the model of the system to predict the future values of the controlling variables over a prediction horizon N. After the prediction of future values it provides the control action sequence by optimizing a user-defined cost function. This algorithm is repeated for every sampling period and the optimized sequence is applied to the system. Usually, the cost function is defined as:

$$g = \sum_{i=0}^{n} \lambda_i |(x_i^* - x_i^p)| \tag{1.1}$$

where $x_i^*$ is the reference value and $x_i^p$ is the predicted value of the controlling variable $x_i$, $\lambda_i$ is the weighing factor and $n$ is the total controlling variables. In this way, multiple variables, constraints and non linearities can be taken into consideration [16].

MPC fulfills the requirement of modern control systems as it considers many system constraints and variables [20]. There are two types of MPC: Continuous Control Set MPC (CCS-MPC) and Finite Set Control MPC (FS-MPC) [21-22]. In CCS-MPC, the continuous output is generated by the controller for the modulator which generates the switching state for the inverter and the controller yields constant switching frequency whereas, in FS-MPC, it directly uses the finite number of control actions available for switching states of the inverter. It does not use the modulator therefore the controller yields variable switching frequency [20].

The design of the FS-MPC has the following ideas:

- Design of the model of the system and to predict the values of the future variables.
- The cost function takes account of all controlling variables and constraints.
- Minimization of the cost function for all the possibilities.

With the help of the system model and all the available information the future values of all the variables till time, $k$ is used to predicted values for sampling time $k + 1$. The cost function is minimized for all the sequences of optimal actuation and then the minimum sequence is applied at the output.

## 1.4 Goal of the Project

The objective of the project is to implement the model predictive control algorithm to control the induction motor fed by the two-level three-phase inverter to achieve a good dynamic response and steady-state response.

## 1.5 Outline

The project work is structured in a manner such that it gives proper theoretical and simulation implementation knowledge.

In chapter 2, the explanation of the three-phase inverter with the equation involved in the implementation is shown. Chapter 3, explains the dynamic modeling of the induction machine. Chapter 4, gives a detailed explanation of the implementation of the PTC scheme which is the brain of the project. Chapter 5, shows the process of implementation of the PTC of induction motor fed by the inverter in MATLAB. Chapter 6, explains the results of various tests performed to test the performance of predictive torque control of induction motor.

# CHAPTER 2

# MODELING OF INVERTER

In this project, a two-level three-phase voltage source inverter (2L-3P-VSI) topology is considered to produce the voltage vectors as shown in Figure 2.1. The 2L-3P-VSI produces two voltage levels of $+V_{dc}$ or $-V_{dc}$ at the output, therefore it is called a two-level voltage source inverter. For each of the three phases, the switching state for each switch $S_a$, $S_b$ and $S_c$ is either '0' or '1' and switching state for each state is complementary which is generated by using logic inversion. The possible switching states for the are shown in table 2.1.

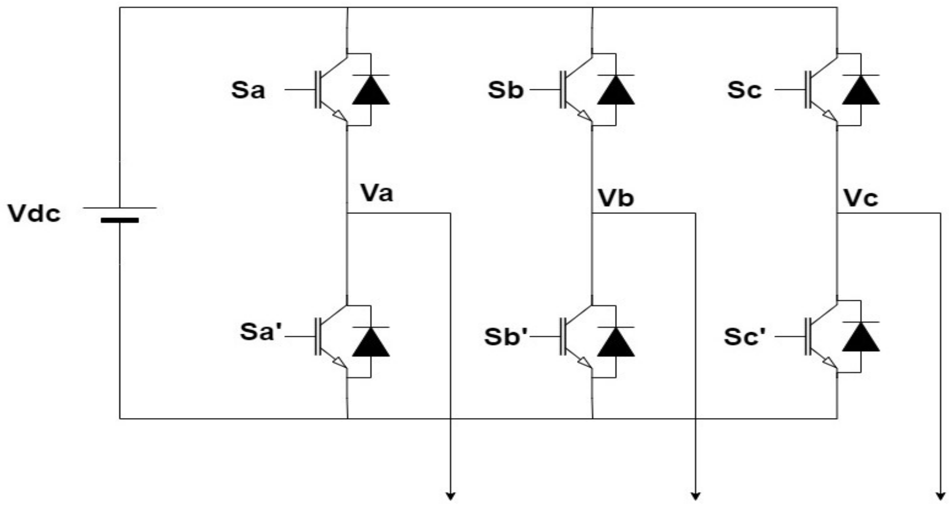


Figure 2.1: Two level three phase inverter

In the term of vector, the three phase switching state can be expressed as

$$\mathbf{S} = \frac{2}{3}(S_a + \mathbf{a}S_b + \mathbf{a}^2 S_c) \tag{2.1}$$

where $a = e^{j\frac{2\pi}{3}}$. The voltage vector generated by the inverter can be given by

$$\mathbf{V} = \frac{2}{3}(V_a + \mathbf{a}V_b + \mathbf{a}^2 V_c) \tag{2.2}$$

where $V_a$, $V_b$ and $V_c$ are the phase voltages.

Table 2.1: Switching State and Voltage vectors

| $\mathbf{S}_a$ | $\mathbf{S}_b$ | $\mathbf{S}_c$ | $\mathbf{V}$ |
|---|---|---|---|
| 0 | 0 | 0 | $\mathbf{V}_0 = 0$ |
| 1 | 0 | 0 | $\mathbf{V}_1 = \frac{2}{3}V_{dc}$ |
| 1 | 1 | 0 | $\mathbf{V}_2 = \frac{1}{3}V_{dc} + j\frac{1}{\sqrt{3}}V_{dc}$ |
| 0 | 1 | 0 | $\mathbf{V}_3 = -\frac{1}{3}V_{dc} + j\frac{1}{\sqrt{3}}V_{dc}$ |
| 0 | 1 | 1 | $\mathbf{V}_4 = -\frac{2}{3}V_{dc}$ |
| 0 | 0 | 1 | $\mathbf{V}_5 = -\frac{1}{3}V_{dc} - j\frac{1}{\sqrt{3}}V_{dc}$ |
| 1 | 0 | 1 | $\mathbf{V}_6 = \frac{1}{3}V_{dc} - j\frac{1}{\sqrt{3}}V_{dc}$ |
| 1 | 1 | 1 | $\mathbf{V}_7 = 0$ |

The 2L-3P-VSI produces 8 voltage vectors corresponding to 8 state vectors at its output terminal as shown in figure 2.2 and possible switching states are shown in table 2.1.

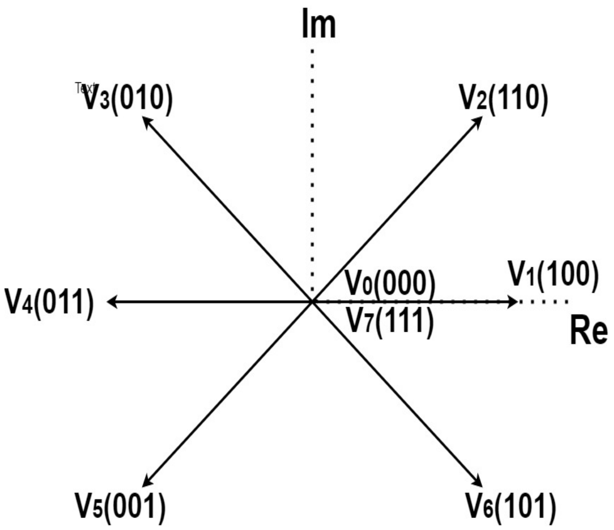


Figure 2.2: Voltage Vectors of two level three phase inverter

This inverter model can include dead time, IGBT saturation, and diode forward voltage drop but in this project, a simple model of the inverter is used for simplicity.

# CHAPTER 3

# DYNAMIC MODELING OF INDUCTION MACHINE

This chapter presents the dynamic modeling of the three-phase squirrel cage induction motor in state space, which analyzes AC circuits easy to understand and implement.

## 3.1 State space representation of the three-phase system to two-axis system

The state-space representation makes an AC circuit simple to represent and easy to understand and analyze. The three-phase AC voltage source $V_a$, $V_b$, and $V_c$, which are located at 120 degrees to each other is supplied to the three phase induction motor [23]. These three phases are linearly dependent on each other, due to which the modeling of the equation becomes complicated. To simply this complication, the three-phase electrical variables such as voltage, current, and flux are modeled properly using a two-axis reference frame. The two-axis representation of the three-phase system is called 'state-space representation'. The two-axis stationary reference frame ($\alpha$-$\beta$) is shown in figure 3.1. The components of the three-phase variable along $a-b-c$ coordinates are projected on $\alpha-\beta$ coordinates. These two coordinates in the $\alpha-\beta$ reference frame are mutually perpendicular to each other and hence linearly independent [24, 25].

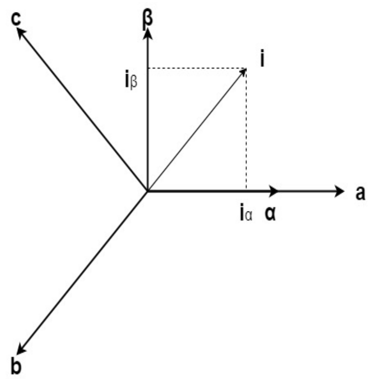


Figure 3.1: State-space two-axis ($\alpha$-$\beta$) representation of three-phase ($a-b-c$) systems

The Clarke transformation is used to convert the three-phase system to a two-axis system using the matrix as shown in the matrix equation for three-phase (a, b, c) current to ($\alpha$-$\beta$).

$$\begin{bmatrix} i_\alpha \\ i_\beta \end{bmatrix} = \begin{bmatrix} 2/3 & -1/3 & -1/3 \\ 0 & 1/\sqrt{3} & 1/\sqrt{3} \end{bmatrix} \begin{bmatrix} i_a \\ i_b \\ i_c \end{bmatrix} \tag{3.1}$$

The state-space representation of Induction Machine variables in ($\alpha$-$\beta$) reference frame are as follows:

$$\mathbf{v}_s = v_{s\alpha} + jv_{s\beta} \tag{3.2}$$

$$\mathbf{v}_r = v_{r\alpha} + jv_{r\beta} \tag{3.3}$$

$$\mathbf{i}_s = i_{s\alpha} + ji_{s\beta} \tag{3.4}$$

$$\mathbf{i}_r = i_{r\alpha} + ji_{r\beta} \tag{3.5}$$

$$\boldsymbol{\varphi}_s = \boldsymbol{\varphi}_{s\alpha} + j\boldsymbol{\varphi}_{s\beta} \tag{3.6}$$

$$\boldsymbol{\varphi}_r = \boldsymbol{\varphi}_{r\alpha} + j\boldsymbol{\varphi}_{r\beta} \tag{3.7}$$

where $\mathbf{v}_s$ and $\mathbf{v}_r$ are stator and rotor voltages, $\mathbf{i}_s$ and $\mathbf{i}_r$ are the stator and rotor currents, $\boldsymbol{\varphi}_s$ and $\boldsymbol{\varphi}_r$ are the stator and rotor flux linkages.

## 3.2 Machine Modeling

The state-space model of a squirrel cage induction machine in $\alpha$-$\beta$ reference frame are shown in the equations below.

$$\mathbf{v}_s = R_s\mathbf{i}_s + \frac{d\boldsymbol{\varphi}_s}{dt} + jw_k\boldsymbol{\varphi}_s \tag{3.8}$$

$$0 = R_r\mathbf{i}_r + \frac{d\boldsymbol{\varphi}_r}{dt} + j(w_k - w_e)\boldsymbol{\varphi}_r \tag{3.9}$$

$$\boldsymbol{\varphi}_s = L_s\mathbf{i}_s + L_m\mathbf{i}_r \tag{3.10}$$

$$\boldsymbol{\varphi}_r = L_m\mathbf{i}_s + L_r\mathbf{i}_r \tag{3.11}$$

$$T_e = \frac{3}{2}pIm(\boldsymbol{\varphi}_s^*\mathbf{i}_s) \tag{3.12}$$

$$J\frac{dw_m}{dt} = T_e - T_l \tag{3.13}$$

where $T_e$ is electromagnetic torque, $T_l$ is external load torque, $p$ is the pole pairs ,$J$ is the moment of inertia of the mechanical shaft.$R_s$ and $R_r$ are the stator and the rotor resistances. $L_s$, $L_r$ and $L_m$ are stator, rotor and magnetizing inductance respectively. $w_k$ is the synchronous speed at which synchronous rotating reference frame rotates with respect to stationary reference frame. $w_m$ is rotor angular speed which is related to the electric rotor speed $w_e$ by the equation:

$$w_e = pw_m \tag{3.14}$$

In equation 3.8, the relationship of stator voltage in terms of stator ohmic drop and stator inductance drop is shown. Since the squirrel-cage rotor is short-circuited, therefore the rotor voltage is zero as shown in equation 3.3. It is convenient to obtain equations of the machine in state variables to develop the best control strategy. The stator current $\mathbf{i}_s$ and rotor flux $\boldsymbol{\varphi}_r$ vectors are selected as state variables. The stator current is specially selected because this variable can be measured and also undesired stator dynamics, like effects on the stator resistance, stator inductance, and back-emf, are avoided. Now we obtain the stator and rotor dynamics of the squirrel cage induction machine from equations 3.8-3.11.

$$i_s + \tau_\sigma \frac{d\mathbf{i}_s}{dt} = -jw_k\tau_\sigma\mathbf{i}_s + \frac{k_r}{R_\sigma}(\frac{1}{\tau_r} - jw_e)\boldsymbol{\varphi}_r + \frac{\mathbf{v}_s}{R_\sigma} \tag{3.15}$$

$$\boldsymbol{\varphi}_r + \tau_r \frac{d\boldsymbol{\varphi}_r}{dt} = -j(w_k - w_e)\tau_r\boldsymbol{\varphi}_r + L_m\mathbf{i}_s \tag{3.16}$$

where $\tau_s = \frac{L_s}{R_s}$, $\tau_r = \frac{L_r}{R_r}$, $\sigma = 1 - \frac{L_m^2}{L_s L_m}$, $k_r = \frac{L_m}{L_r}$, $k_s = \frac{L_m}{L_s}$ and $R_\sigma = R_s + R_r k_r^2$.

# CHAPTER 4

# Predictive Torque Control of Induction Motor fed by Two Level Inverter

In the previous chapter, dynamic equations of the induction motor and two-level three-phase inverter are shown which will help in implementing the PTC scheme since it used both models of induction machine and inverter explicitly. The basic idea of PTC is taken from Direct Torque Control (DTC) in which we can modify electromagnetic torque **T** and stator flux $\varphi_s$ by selecting the proper voltage vector sequence for the inverter to change the magnitude of stator flux and at the same time change the angle between rotor and stator flux. The same principle is used in PTC, but here we predict the future values of electromagnetic torque and stator flux with respect to the reference values for every actuating possibility and then the cost function selects the voltage vector which optimizes the predicted values with the reference values.

An FS-PTC model is implemented in three steps: Stator and rotor flux estimation, Torque and flux prediction, and cost function minimization as shown in figure 4.1.

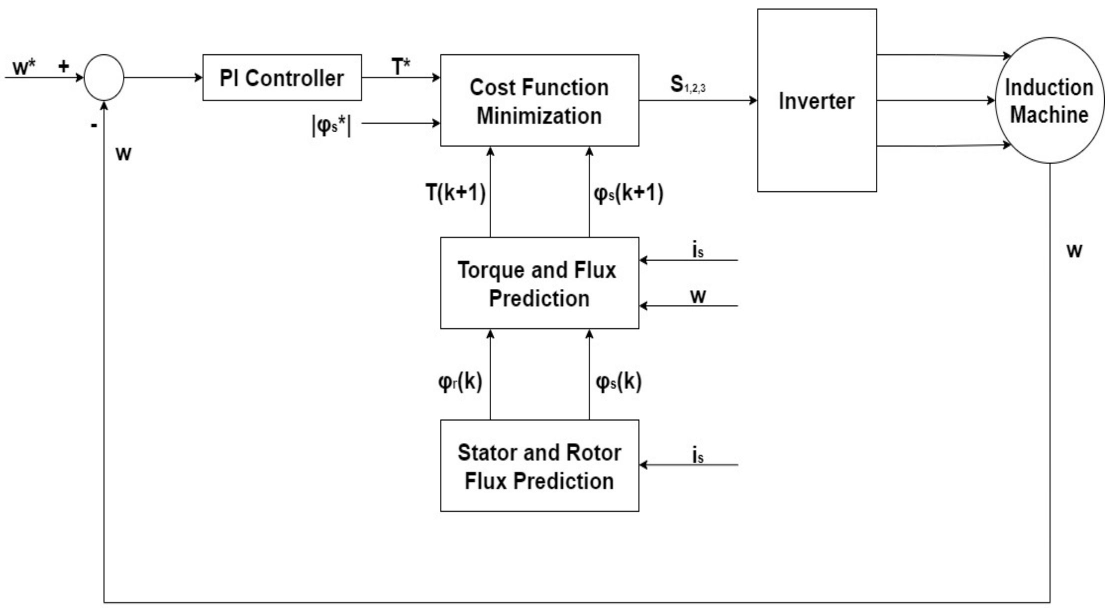


Figure 4.1: Predictive Torque Control Scheme

## 4.1 Estimation

In the FS-PTC model shown in figure the Stator and rotor flux estimation block, the values stator flux $\boldsymbol{\varphi}_s$ and the rotor flux $\boldsymbol{\varphi}_r$ is estimated at present sampling time.

The estimation of values of stator flux $\hat{\boldsymbol{\varphi}}_s(k)$ is done using the stator voltage equation 3.8. Since FS-PTC is modeled in stationary reference frame therefore $w_k$ is set to zero. So the equation 3.8 becomes:

$$\mathbf{v}_s = R_s\mathbf{i}_s + \frac{d\boldsymbol{\varphi}_s}{dt} \tag{4.1}$$

The discretization of the above equation is done using Euler approximation formula as:

$$\frac{d\boldsymbol{\varphi}_s}{dt} = \frac{\boldsymbol{\varphi}_s(k) - \boldsymbol{\varphi}_s(k-1)}{T_s} \tag{4.2}$$

where $T_s$ is the sampling time period.

Now, using equation 4.2 in equation 4.1, we can obtain the estimated value of stator flux at present sampling time $\boldsymbol{\varphi}_s(k)$.

$$\hat{\boldsymbol{\varphi}}_s(k) = \hat{\boldsymbol{\varphi}}_s(k-1) + T_s v_s(k) - R_s T_s i_s(k) \tag{4.3}$$

The estimation of rotor flux $\hat{\boldsymbol{\varphi}}_r(k)$ is obtained from the flux linkage equations 3.10 and 3.11. By replacing $\mathbf{i}_r$ from equation 3.10 in equation 3.11 we obtain the rotor flux as:

$$\boldsymbol{\varphi}_r = \frac{L_m}{L_r}\boldsymbol{\varphi}_s + (L_m - \frac{L_s L_r}{L_m})\mathbf{i}_s \tag{4.4}$$

The discretization of the above equation is done as:

$$\hat{\boldsymbol{\varphi}}_r = \frac{L_m}{L_r}\hat{\boldsymbol{\varphi}}_s + (L_m - \frac{L_s L_r}{L_m})\mathbf{i}_s \tag{4.5}$$

## 4.2 Prediction

After the estimation of stator and rotor flux, the prediction of stator flux and torque for the next sample instant (k+1) is required as they are the controlling variables for PTC.

For the prediction of the stator flux, we use the same stator voltage equation used for estimation. Therefore, we approximate the derivative of stator flux using the Euler approximation formula as in stator voltage equation 4.2. The equation obtained is:

$$\boldsymbol{\varphi}_s^p(k+1) = \hat{\boldsymbol{\varphi}}_s(k) + T_s v_s(k) - R_s T_s i_s(k) \tag{4.6}$$

'p' in superscript depict the predicted stator flux variable. For the prediction of electromagnetic torque $T^p(k+1)$ we need stator flux $\boldsymbol{\varphi}_s^p(k+1)$ and stator current $\mathbf{i}_s^p(k+1)$ is required. Stator flux $\boldsymbol{\varphi}_s^p(k+1)$ we can get from equation from equation 4.6.

For the prediction of stator current, we discretize equation 3.15 using Euler-based approximation. The equation obtained for stator current at time instant (k+1) is:

$$\mathbf{i}_s^p(k+1) = (1 - \frac{T_s}{\tau_\sigma})\mathbf{i}_s(k) + \frac{T_s}{(\tau_\sigma + T_s)}[\frac{1}{R_\sigma}((\frac{k_r}{\tau_r} - jk_r w_e)\hat{\boldsymbol{\varphi}}_r(k) + \mathbf{v}_s(k))] \tag{4.7}$$

Electromagnetic Torque $T_e$ prediction depends on the the stator flux and the stator current as:

$$T_e = \frac{3}{2} p Im[\bar{\boldsymbol{\varphi}}_s \mathbf{i}_s] \tag{4.8}$$

After the prediction of stator flux and and stator current, prediction of electromagnetic torque can be done using the equation:

$$T_e^p(k+1) = \frac{3}{2} p Im[\bar{\boldsymbol{\varphi}}_s(k+1)\mathbf{i}_s(k+1)] \tag{4.9}$$

## 4.3 Cost Function Minimization

The predicted variables are evaluated by a predefined cost function which helps in switching state selection. In FS-PTC, we generally include the absolute difference of the reference and predicted values. The cost function defined for PTC of induction machine can be defined as

$$g = |T_e^*(k+1) - T_e^p(k+1)| + \lambda_\varphi |\boldsymbol{\varphi}_s^*(k+1) - \boldsymbol{\varphi}_s^p(k+1)| \tag{4.10}$$

where $T_e^*(k+1)$ and $\boldsymbol{\varphi}_s^*(k+1)$ are reference electromagnetic and stator flux values. $T_e^p(k+1)$ and $\boldsymbol{\varphi}_s^p(k+1)$ are predicted values of electromagnetic and stator flux at (k+1) time instant. $\lambda_\varphi$ is the weighting factor which helps in increasing or decreasing the relative importance of stator flux with respect to electromagnetic torque. The value of the weighing factor is taken as nominal values of torque and stator flux.

$$\lambda_\varphi = \frac{T_n}{|\Phi_{sn}|} \tag{4.11}$$

This cost function $g$ is evaluated for every voltage vector. The minimum cost function out of all the voltage vectors is selected and the respective switching state feeds into the three-phase inverter.

# CHAPTER 5

# Implementation

In this chapter, the implementation of the PTC scheme of induction machine fed by the two-level three-phase inverter as a simulation in MATLAB is shown for different blocks as shown in figure 5.1.

Figure 5.1 shows the Simulink model used for simulation. This model contains mainly 6 blocks as Speed Reference, PI Controller, Predictive Controller, Inverter, $abc$ to $\alpha - \beta$ conversion, and induction machine model.

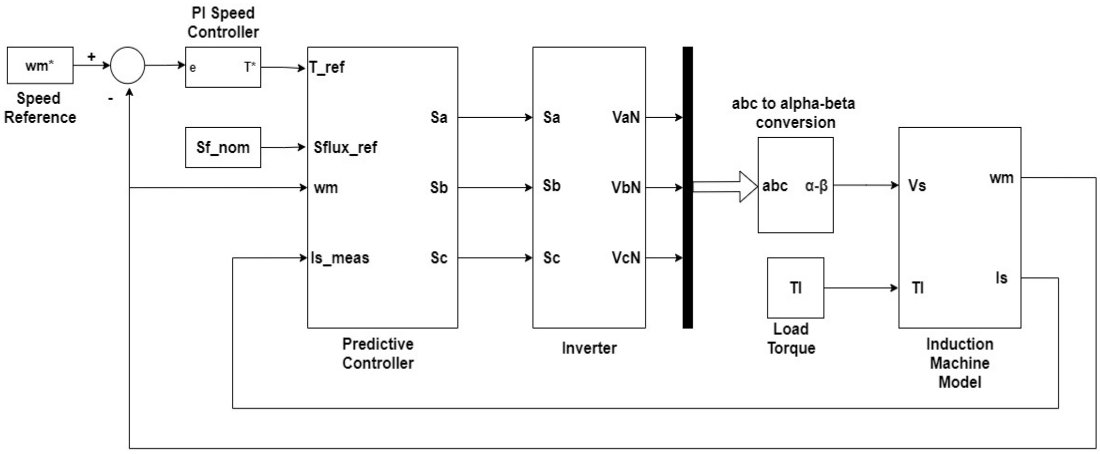


Figure 5.1: Simulink model for PTC of Induction Machine

## 5.1 PI Controller

The reference speed can be a constant or a step as per the requirement which is compared to the measured speed and error is generated. This error is fed to the discrete-time PI Speed Controller to compute the electromagnetic torque reference values. The value to two tuning parameters Kp (proportional gain) and Ki (integral gain) are shown in table 5.1. For the design of the parameters, the transfer function between the speed of the rotor and electrical torque is obtained as:

$$\frac{w_m(s)}{T_e(s)} = \frac{1}{Js} \tag{5.1}$$

Table 5.1: PI Controller Parameters

| PI Controller Parameters | Values |
|---|---|
| $K_p$ | 50.16 |
| $K_i$ | 2.56 |

A saturation block is implemented in the PI controller to keep the torque values within the limits.

## 5.2 Predictive Controller

The predictive controller takes reference torque, reference stator flux, measured speed, and measured stator current as the input and produces the three switching states $S_a$, $S_b$ and $S_c$ which are applied as gating signals to the inverter. This predictive controller is implemented as the algorithm in MATLAB FUNCTION BLOCK.

## 5.3 Inverter

The inverter takes the gating signal as input and generates a three-phase voltage at the output. The DC link is assumed as the ideal DC source and this voltage is directly multiplied by the gating signal as power semiconductors are modeled as ideal switches. The implementation of the inverter can be seen in figure 5.2.

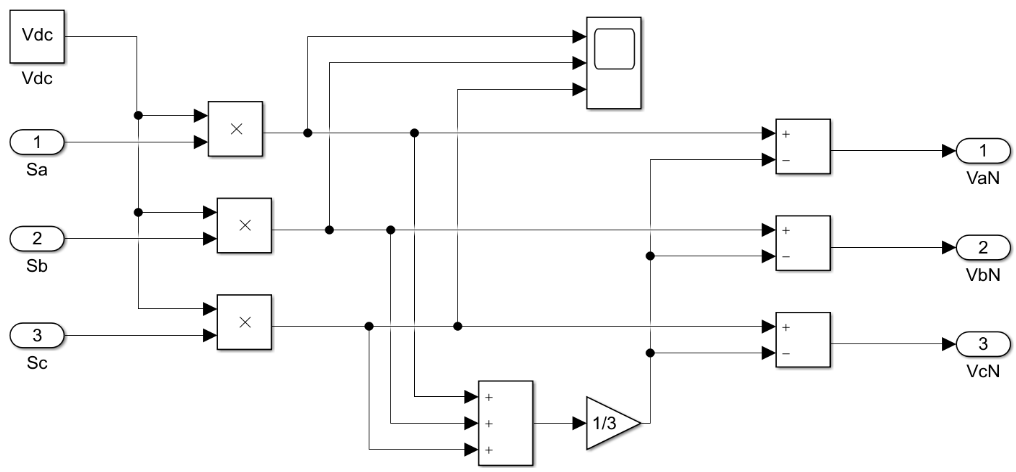


Figure 5.2: Implementation of Three Phase Inverter in Simulink

## 5.4 Induction Machine

The induction machine used in this model is in $\alpha - \beta$ frame, therefore the three-phase voltage is converted in $\alpha - \beta$ as explained in equation 3.2. The induction machine block takes stator voltage in $\alpha - \beta$ frame and load torque as input and generated stator current and rotor speed as output. The implementation of the induction machine model is shown in figure 5.3.

The induction machine modeling equations obtained in section 3.2 are used in the implementation. The motor specifications are mentioned in table 5.2.

Table 5.2: Motor Specifications

| SPECIFICATION | VALUE |
|---|---|
| Power (P) | 6000 W |
| Voltage (Vdc) | 520 V |
| Frequency (f) | 50 Hz |
| Number of poles (P) | 2 |
| Rated speed (N) | 2860 rpm |
| Stator Resistance ($R_s$) | 1.2 Ω |
| Rotor Resistance ($R_r$) | 1 Ω |
| Stator Inductance ($L_s$) | 0.175 H |
| Rotor Inductance ($L_r$) | 0.175 H |
| Mutual Inductance ($L_m$) | 0.170 H |
| Inertia constant (J) | 0.062 Kg-$m^2$ |

From the power and torque relation, we can evaluate rated torque as:

$$T_{rated} = \frac{P_{rated}}{N_{rated}} \tag{5.2}$$

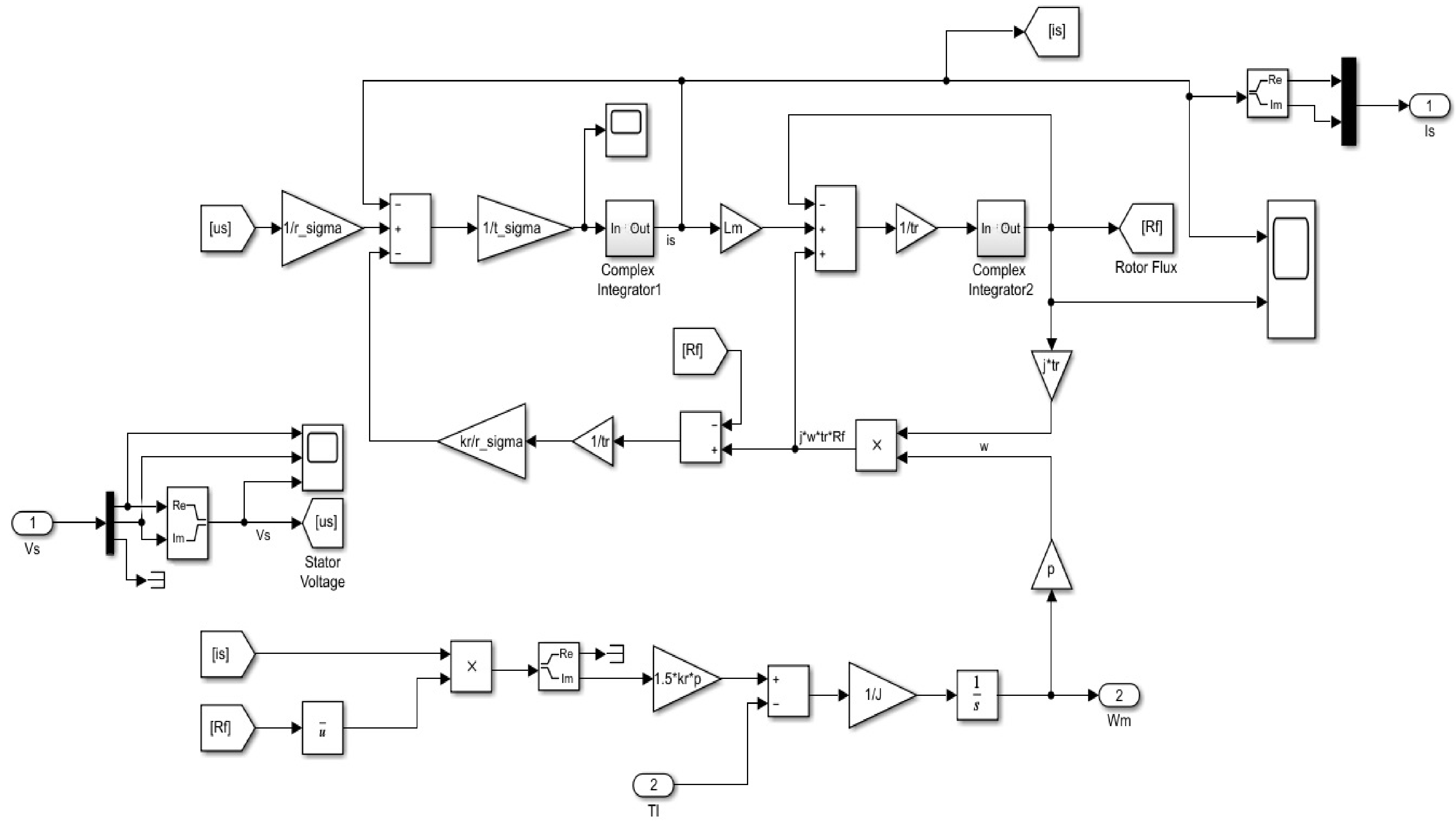


Figure 5.3: Implementation of Induction Machine in Simulink

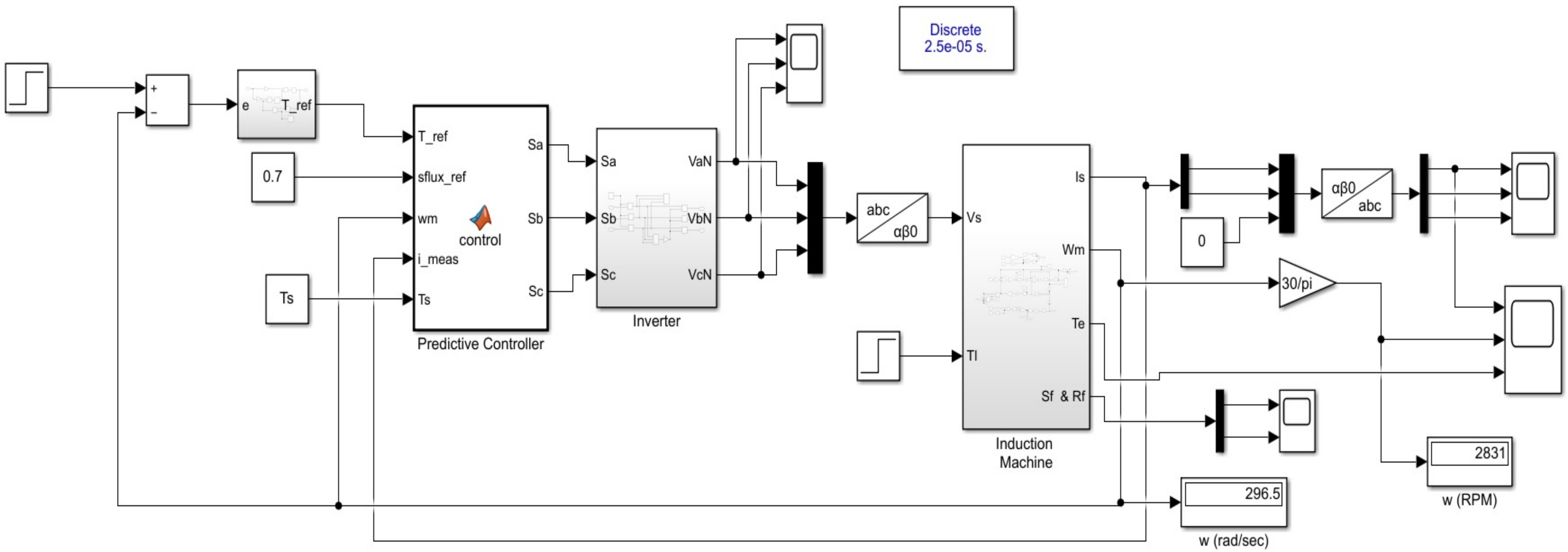


Figure 5.4: Simulink Model of Predictive Torque Control of Induction Motor fed by the Two Level Three Phase Inverter

# CHAPTER 6

# Results

The FS-PTC scheme was implemented in MATLAB as shown in the previous chapter and various tests were performed to test the performance of the induction motor and parameters are shown in table 5.2 at a sampling frequency of 40 kHz. In this simulation, the behavior of the system at four different conditions i.e starting response, speed reversal response, load test response, and steady-state response is shown in Figures 6.1 to 6.8. The rated speed of the rotor is 2860 RPM with nominal load torque of 20 Nm.

## 6.1 Starting Response

The starting response is presented for the induction motor firstly. In this, the reference speed command is set as step command which increases from 0 to rated speed i.e. 2860 RPM at t = 0.5 seconds, and the response of stator current, speed, and electromagnetic torque are shown in figure 6.1.

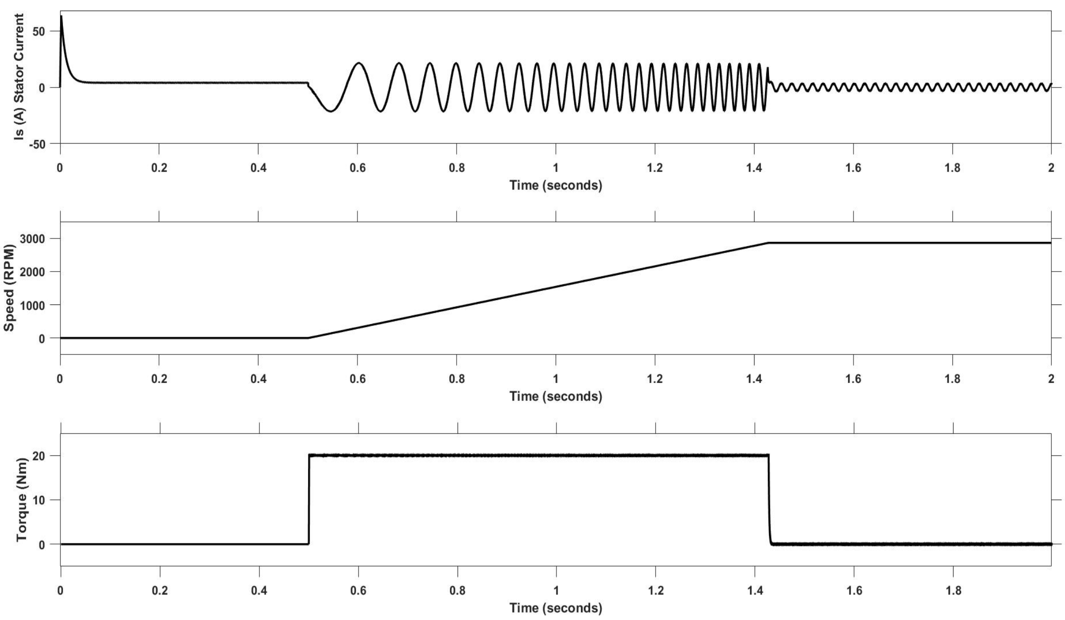


Figure 6.1: Stator current, speed and torque starting response waveform of PTC.

As the speed is set to increase at t = 0.5 seconds, the torque quickly changes from zero to the nominal value and allows the rotor to accelerate and the rotor smoothly

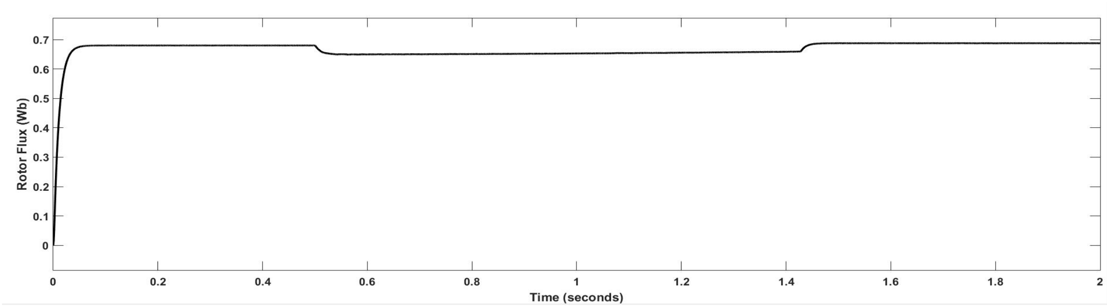


Figure 6.2: Rotor Flux waveform during starting response of PTC.

reaches the rated speed. After reaching the reference speed, torque reduces to zero. During the change in the rotor speed, a little dip can also be observed in rotor flux as shown in figure 6.2.

## 6.2 Speed Reversal

The drive is tested for speed reversal. At zero external load torque condition, the speed reference command is set to change the rotor speed from +2860 RPM to -2860 RPM at t = 2 seconds. The results for the stator current, speed, and torque are shown in figure 6.3.

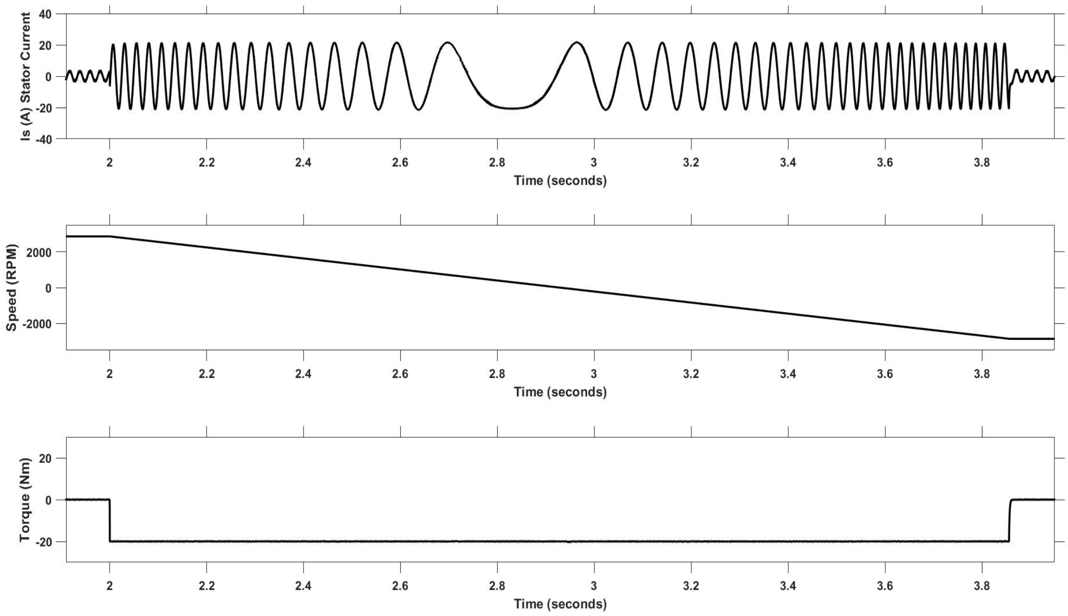


Figure 6.3: Stator current, speed and torque waveform of PTC in speed reversal.

When the speed reference command is set to -2860 at t = 2 seconds, the torque immediately changes from zero to negative nominal value i.e 20 Nm to allow deceleration of the rotor speed and remains at the same value till the rotor reaches the reference speed and after that, it again increases to zero.

## 6.3 Load Test

In this load test, firstly the motor is set to run at the rated speed and suddenly the load torque is changed from zero to the rated torque of 20 Nm at t = 2 seconds. The results for stator current, speed, and torque for load test are shown in figure 6.4.

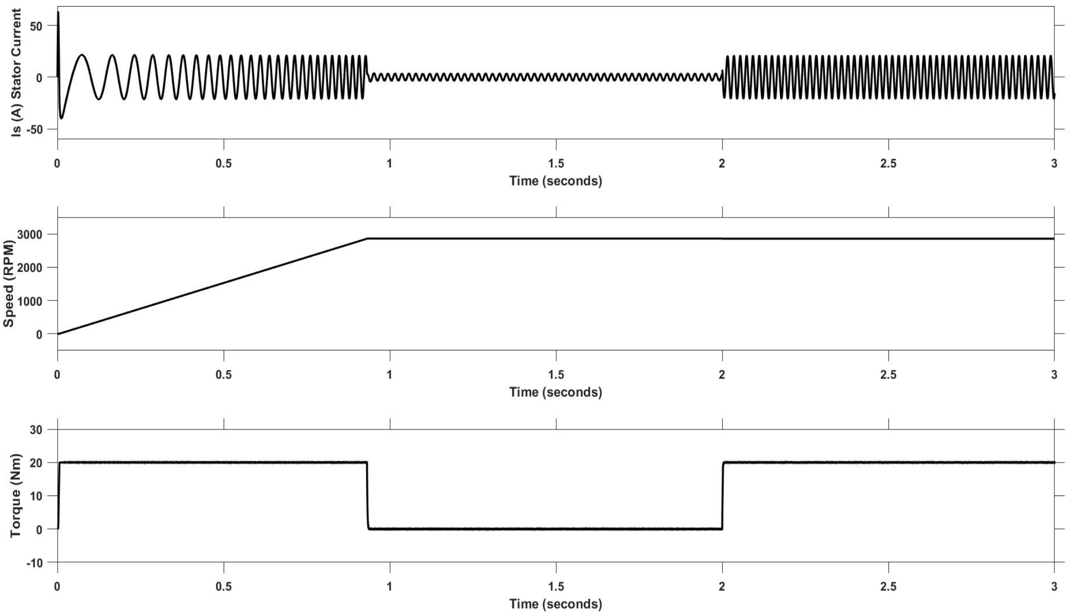


Figure 6.4: Stator current, speed and torque waveform of PTC in load test.

At t = 2 seconds, it can be seen that the torque increases to the nominal value to meet the requirements in the increase in the load torque. Also, a small decrease in the rotor speed can be observed in the change of the load torque. The stator current can be seen to be increased on the increase of torque values. The fast dynamic response of the system can be seen as torque changes from 0 Nm to 20 Nm in 2.4 milliseconds as shown in figure 6.5.

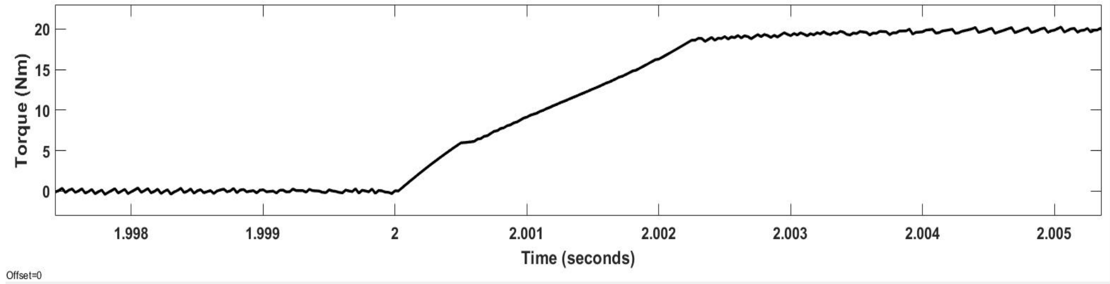


Figure 6.5: Electromagnetic torque response at load test condition of PTC.

## 6.4 Steady State Behavior

In this test, the reference speed command is set to the rated speed of 2860 RPM and a load torque of 10 Nm. The THD of stator current in figure 6.6 and torque ripple is observed as shown in figures 6.7 and 6.8 respectively. Lower harmonic distortion was observed in stator current as the resulting THD is 4.47 % in figure 6.7. The peak to peak ripple observed in the torque response is 0.86 Nm.

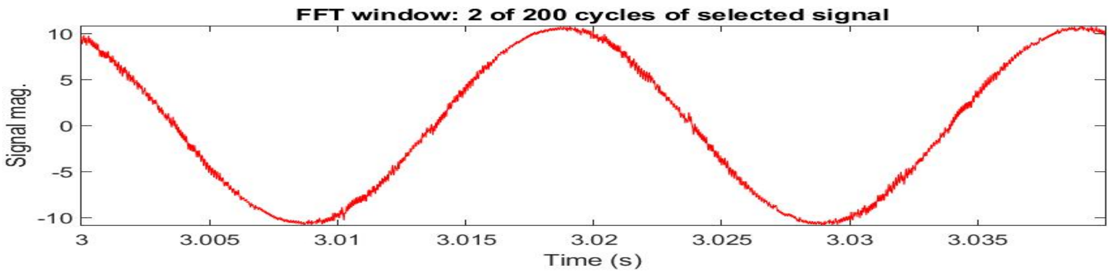


Figure 6.6: Stator current waveform of PTC in steady state.

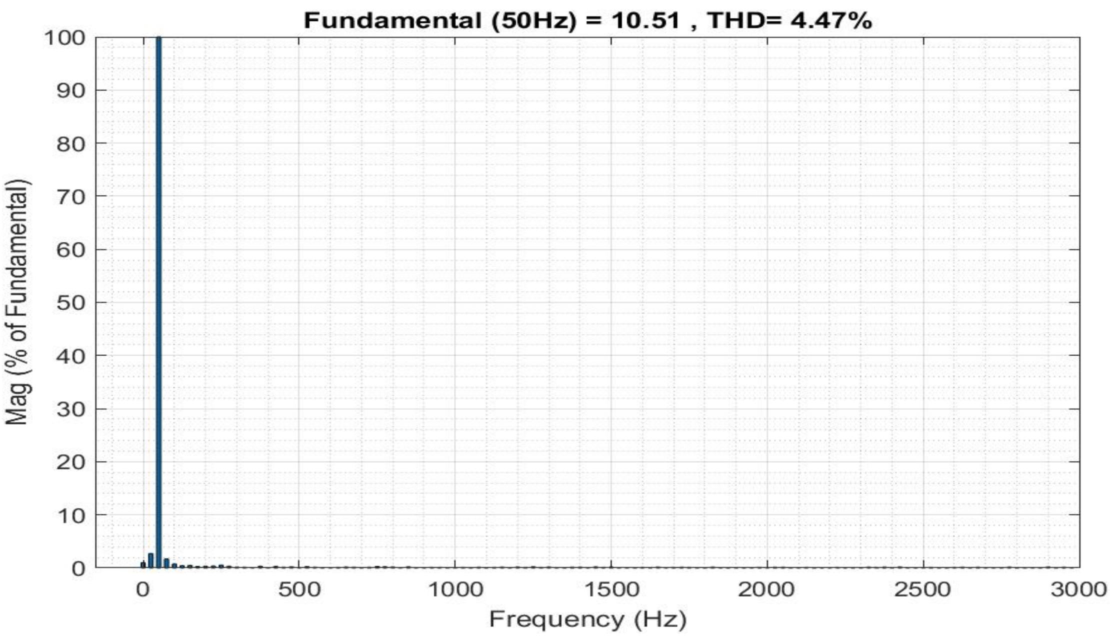


Figure 6.7: THD at given load conditions

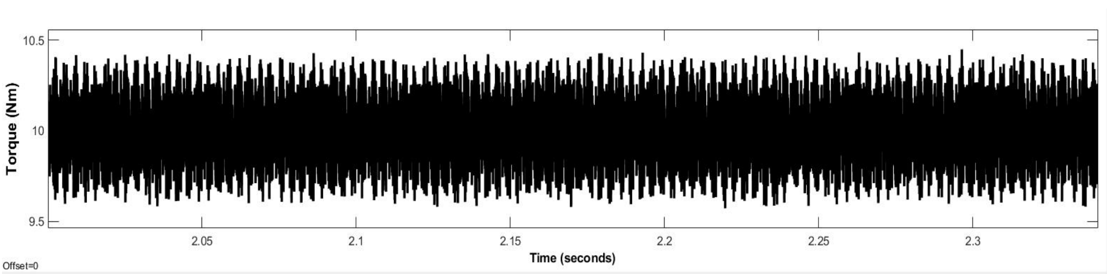


Figure 6.8: Electromagnetic torque ripple waveform of PTC in the steady state.

# CHAPTER 7

# Conclusion

In this report, the model predictive control of the induction machine is discussed. Various classical control techniques are available like FOC and DTC and their advantages and disadvantages are also discussed in this report. The report demonstrates that predictive control is powerful and flexible for the designing of the controllers. Its advantages like fast dynamics, easy inclusion of constraints and non-linearities can be observed which makes it suitable for the control of the power converters and motor drives.

This project explains the application of the MPC technique in an induction motor fed by a two-level three-phase inverter. The basic principle of PTC and its application on induction motors is explained in detail which is the prominent predictive control method. The state-space model of the induction motor and inverter is explained with their model used in implementing the PTC. The systematic process of evaluation of the cost function is shown to select the proper switching voltage vector.

The PTC method has an intuitive method and easy implementation. It does not require any inner PI controller and the modulator is also not needed in its implementation, which results in faster dynamics but with variable switching frequency. Various tests performed on the FS-PTC model explained the good performance of the induction motor in terms of torque, flux, stator current THD, robustness against load torque disturbance, and step torque response. The system performs well in both steady and transient states with good tracking of reference values, reduced torque ripple, and lower total harmonic distribution in the steady-state response.

# REFERENCES


1. Model Predictive Control—A Simple and Powerful Method to Control Power Converters by Samir Kouro, IEEE Transactions on Industrial Electronics, Year: 2008, Pages: 1826 - 1838.

2. W. Slabiak and L. J. Lawson. Precise control of a three-phase squirrel-cage induction motor using a practical cycloconverter. IEEE Transactions on Industry and General Applications, IGA-2(4):274–280, July 1966.

3. Riveros J.A., Barrero F., Levi E., Duran M.J., Toral S. and Jones M. 'Variable-speed five-phase induction motor drive based on predictive torque control'. IEEE Trans. on Ind. Electronics. 2013; 60(8): 2957–2968.

4. Casadei D., Profumo F., Serra G. and Tani A. 'FOC and DTC: two viable schemes for induction motors torque control'. IEEE Trans. Power Electronics. 2002; 17(5): 779–787.

5. Takahashi I. and Noguchi T. 'A new quick-response and high-efficiency control strategy of an induction motor'. IEEE Trans. on Ind. Applications. 1986; IA-22(5): 820–827.

6. Depenbrock M. 'Direct self-control (DSC) of inverter-fed induction machine'. IEEE Trans. on Power Electronics. 1988; 3(4): 420–429.

7. Vas P. Sensorless vector and direct torque control. New York: Oxford Univ. Press, 1998.

8. G.-A. Capolino, "Recent advances and applications of power electronics and motor drives–advanced and intelligent control techniques," in 34th Annual IEEE Conference on Industrial Electronics, IECON. pp. 37–39, November 2008.

9. P. Cortes, M. P. Kazmierkowski, R. M. Kennel, D. E. Quevedo, and J. Rodrıguez, "Predictive control in power electronics and drives," IEEE Transactions on Industrial Electronics, vol. 55, no. 12, pp. 4312–4324, December 2008.

10. T. Kawabata, T. Miyashita, and Y. Yamamoto, "Dead beat control of three phase PWM inverter," IEEE Transactions on Power Electronics, vol. 5, no. 1, pp. 21–28, January 1990.

11. O. Kukrer, "Discrete-time current control of voltage-fed three-phase PWM inverters," IEEE Transactions on Industrial Electronics, vol. 11, no. 2, pp. 260–269, March 1996.

12. J. Holtz and S. Stadtfeld, "A predictive controller for the stator current vector of AC machines fed from a switched voltage source," in International Power Electronics Conference, IPEC, Tokyo, pp. 1665–1675, 1983.

13. P. Mutschler, "A new speed-control method for induction motors," in Conference Record of PCIM'98, Nuremberg, pp. 131–136, May 1998.

14. Garcia C.E., Prett D.M. and Morari M. ‘Model predictive control: theory and practice – a survey’. Automatica. 1989; 25(3): 335–348.

15. Maciejowski J.M. Predictive control with constraints. Englewood Cliffs, NJ: Prentice Hall, 2002.

16. Goodwin G.C., Seron, M.M. and Dona J.A.D. Constrained control and estimation – an optimization perspective. Berlin: Springer Verlag, 2005.

17. Vazquez S., Rodriguez J., Rivera M., Franquelo L.G. and Norambuena M. ‘Model predictive control for power converters and drives: advances and trends’. IEEE Trans. on Ind. Electronics. 2017; 64(2): 935-947.

18. Papafotiou G.A., Demetriades G.D. and Agelidis V.G. ‘Technology readiness assessment of model predictive control in medium- and high-voltage power electronics’. IEEE Trans. Ind. Electronics. 2016; 63(9): 5807–5815.

19. Rodriguez J. and Cortes P. Predictive control of power converters and electrical drives. Chichester: Wiley, 2012.

20. Kouro S., Cortes P., Vargas R., Ammann U. and Rodriguez J. ‘Model predictive control—a simple and powerful method to control power converters’. IEEE Trans. on Ind. Electronics, 2009; 56(6): 1826–1838.

21. Kouro S., Cortes P., Vargas R., Ammann U. and Rodriguez J. ‘Model predictive control—a simple and powerful method to control power converters’. IEEE Trans. on Ind. Electronics, 2009; 56(6): 1826–1838.

22. Cortes P., Ortiz G., Yuz J.I., Rodriguez J., Vazquez S. and Franquelo L.G. ‘Model predictive control of an inverter with output LC filter for UPS applications’. IEEE Trans. on Ind. Electronics. 2009; 56(6): 1875–1883.

23. Miranda H., Cortes P., Yuz J.I. and Rodriguez J. ‘Predictive torque control of induction machines based on state-space models’. IEEE Trans. on Ind. Electronics. 2009; 56(6): 1916–1924.

24. Cortes P., Rodriguez J., Silva C. and Flores A. ‘Delay compensation in model predictive current control of a three-phase inverter’. IEEE Trans. on Ind. Electronics. 2012; 59(2): 1323–1325.

25. Holtz J. ‘The dynamic representation of ac drive systems by complex signal flow graphs’. Symposium Proceedings in Industrial Electronics, 1994, ISIE’94; 1994. pp. 1–6.